International Journal of Nanoelectronics and Materials
Volume 13, No. 1, Jan 2020 [63-70]

Synthesis of Calcium Phosphate: Influence of Sintering Temperature on the Formation of Fluorhydroxyapatite

Zudah Sima'atul Kubro[1,2], Setyanto Tri Wahyudi[1] and Kiagus Dahlan[1,2*]

[1]*Division of Biophysics, Department of Physics, Bogor Agricultural University, Bogor, Indonesia 16680.*
[2]*Advanced Research Laboratory, Bogor Agricultural University, Bogor, Indonesia 16680.*

Received 13 March 2019, Revised 9 July 2019, Accepted 8 October 2019

ABSTRACT

Calcium phosphate biomaterials can be classified as polycrystalline ceramics. Hydroxyapatite is one kind of calcium phosphate biomaterials which is also a mineral component in hard tissue, especially dental and bones. Hydroxyapatite has low chemical stability at high temperatures and low durability in an acidic environment. On the other hand, fluorhydroxyapatite has good chemical stability at high temperatures as well as the nature of its bioactivity. Fluorhydroxyapatite is made by adding F to replace some OH functional groups in hydroxyapatite. In this research, fluorhydroxyapatite was synthesized through precipitation method and microwave assistant with sintering temperatures of 600°C, 800°C, and 1000°C. Based on the characterization using an x-ray diffractometer, the results showed that at 1000°C sintering temperature, the samples have a higher intensity of fluorapatite and fewer impurities than other samples sintered at 800°C and 600°C. Fourier Transform Infra-Red (FTIR) analysis shows that similar functional groups appeared in the samples with all sintering temperatures. Conductivity evaluation shows that the conductivity values of the samples were inversely proportional to the sintering temperatures. The morphology of the samples not so clearly seen due to agglomeration, but it can be observed that fluorhydroxyapatite is flat-shaped needle-like or rod-shaped.

Keywords: Calcium Phosphate, Fluorhydroxyapatite, Sintering Temperature.

1. INTRODUCTION

Calcium phosphate materials are widely applied as biomaterials [1], adsorbents [2], materials for drug delivery [3], materials in chemical engineering and agriculture [4], and fiber reinforcement [5, 6, 7]. All calcium phosphate compound that is currently developed has a polycrystalline structure. This structure is derived from single-crystals which are very easily oxidized, then form crystalline grains through the sintering processes [8]. Among these are hydroxyapatite [9], beta-tricalcium phosphate [10], tricalcium phosphate [11] and calcium phosphate itself [12].

Hydroxyapatite is one kind of calcium phosphate functioning as a mineral component in hard tissue, especially dental and bone tissue [13, 14, 15]. Synthetic hydroxyapatite is a biomaterial that is most often used in the field of biomaterial science, to repair hard tissue [14] such as teeth and bones due to its osteoconductive [15, 16] and high bioactive properties [17]. On the other hand, hydroxyapatite has low chemical stability at high temperatures. This is indicated by the appearance of other phases besides hydroxyapatite such as tricalcium phosphate and octa calcium phosphate [18]. High dissolution conditions in a biological environment and low resistance to damage in an acidic environment are also other characteristics of hydroxyapatite [13].

Corresponding Author: kdahlan@apps.ipb.ac.id*

Fluorhydroxyapatite is a very unique material. This material is basically hydroxyapatite but some OH functional groups are replaced by F ions. Hydrogen ions contained in hydroxyapatite are in the gap of atoms adjacent to oxygen ions so that they form OH-groups that are randomly oriented causing a disturbance in the hydroxyapatite structure. When this OH-group is partially substituted by F ions, they will produce a neatly arranged apatite structure that increases chemical stability and thermal stability of the apatite structure. When the F ion concentration in the fluorhydroxyapatite reaches 50%, this causes a loss of interference with the hydroxyapatite crystal structure [18]. Hence, making the fluorhydroxyapatite a promising material for increasing the stability properties of hydroxyapatite in biomedical applications [14, 19]. In its development, fluor is one of the most studied material in dental restoration problems because of its nature which can prevent dental caries caused by bacteria and acidic environments [20]. In addition, fluor can also increase mineralization and crystallization in bone formation [13, 20, 21].

Fluorhydroxyapatite can be synthesized by several methods such as wet chemical technique [18], solid-state reaction [22], pH-cycling method [23], plasma spray process [19], mechanochemical reaction [24] and sol-gel [25]. In this study, we reported synthesize and characterization of fluorhydroxyapatite through precipitation method and microwave assistant with a range of sintering temperatures. The use of microwaves in the synthesis of fluorhydroxyapatite may increase efficiency and, therefore, reduce the cost. This method is effective and selective since the power and holding time may be varied so that affects the speed of reaction [26]. The sintering process is the most important part because it plays a role in the density of fluorine in the formation of fluorhydroxyapatite [27]. Therefore, variations in sintering temperatures are needed to determine the most optimum sintering temperatures in the synthesis of fluorhydroxyapatite.

2. EXPERIMENTAL SECTION

2.1 Materials and Methods

Synthesis of fluorhydroxyapatite was carried out using the precipitation method. CaO powder obtained from the calcination of chicken eggshells [28] was deposited into a beaker glass and 100 ml distilled water was added to make 0.5 M concentration. 0.3 M H_3PO_4 solution was mixed with NH_4F solution with a molarity ratio [P]/[F] of 4. In order to obtain the composition of $Ca_{10}(PO_4)_6F_{1.5}OH_{0.5}$, a total of 50 ml of 0.3 M H_3PO_4 and 50 ml of NH_4F solution were then dropped into CaO suspension accompanied by a stirring process during the precipitation process at a speed of 300 rpm. Then the suspension was put into a microwave oven and exposed to 200 W microwave irradiation for 45 minutes. After the microwave irradiation processes, the samples were then dried at 100°C using a furnace for 45 minutes and then sintered with variations in sintering temperatures of 600°C, 800°C, and 1000°C for 2 hours.

2.2 Analysis and Characterization

Samples obtained were characterized and analyzed using XRD, FTIR, SEM and LCR Meters. X-ray diffractometer (X-ray diffraction (XRD) Shimadzu XRD-7000, and Rigaku MiniFlex) was used to determine the phase and parameters of the lattice. The data taken are in the 2θ interval of 10° to 80° with a scan speed of 0.05 and time per step of 1 second. Data obtained from XRD analysis are in the form of diffraction peaks which are then matched with literature data, namely the Joint Committee on Powder Diffraction Standard (JCPDS) numbers 15-0876 (Fluorapatite) and number 09-0432 (Hydroxyapatite). It is worth mentioning that the fluorhydroxyapatite structure shown in the XRD results is the transition structure from hydroxyapatite to fluorapatite. Unfortunately, the structure of carbonate substituted by F is not found in the ICDD database [18]. Fourier transform infrared spectroscopy analysis using Perkin Elmer Spectrum One FT-IR Spectrometer was carried out by means of 1 mg of the sample mixed with 300 mg KBr and then

formed into transparent pellets. These pellets were then analyzed using FTIR with a wavenumber range of 400 to 4000 cm^{-1}.

Samples that will be characterized using SEM firstly should be coated with gold using the sputtering method. The sample was then tested using SEM (JEOL JSM-6510LA) with an acceleration voltage of 15 kV. Conductivity of the samples was measured by using a HiTESTER 3522-50 LCR Meter. The measurement was carried out using a frequency interval of 50 Hz to 5 MHz. The sample to be tested was placed between two electrodes. The electrode was connected to the LCR meter for scanning using the probe.

3. RESULTS AND DISCUSSION

3.1 The XRD Characterization

Figure 1 shows the XRD patterns of the samples. From the figure, it can be seen that all samples show the presence of the fluorapatite phase but with different intensities. The higher sintering temperature shows the fluorapatite phase dominates. This proves that fluorine ions have substituted some of the hydroxyl groups in hydroxyapatite to form fluorhydroxyapatite [14]. It may be said that the fluorhydroxyapatite structure shown in the XRD results is the transition structure from hydroxyapatite to fluorapatite. Unfortunately, the structure of carbonate substituted by F is not found in the JCPDS database.

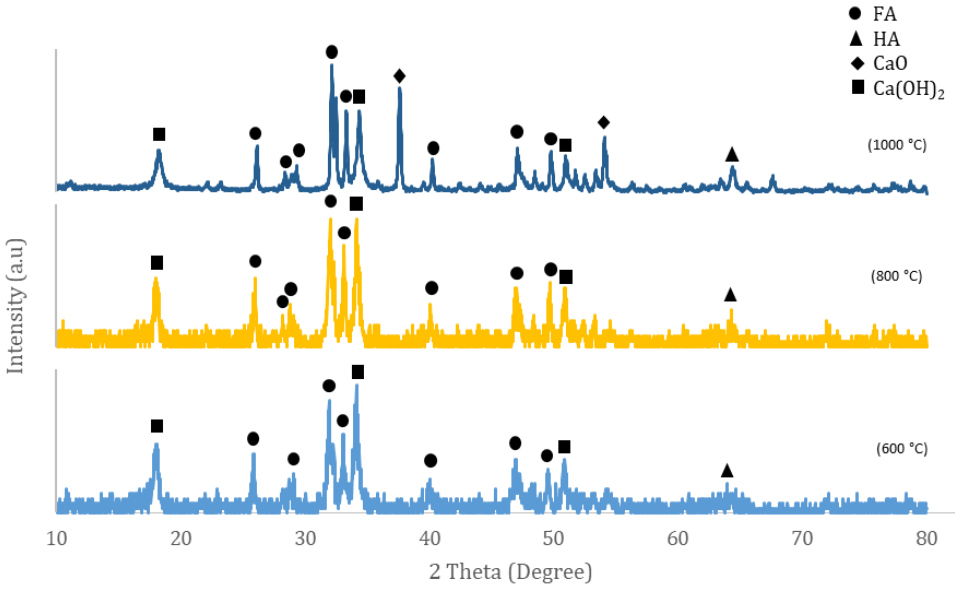

Figure 1. XRD spectra for all samples with variations in sintering temperatures of 600°C, 800°C, and 1000°C.

The $Ca(OH)_2$ phase appears from the three samples with high intensity. For samples with the 600°C sintering temperature, the highest peaks owned by $Ca(OH)_2$, although the majority phase is still owned by the fluorapatite. The $Ca(OH)_2$ phase in each sample decreases in intensity as the sintering temperature increases. It shows that the higher the sintering temperature used, the more fluoride ions will replace the hydroxyl group. In addition, the CaO phase also appears in the sample. Actually, this phase also exists in all samples as $Ca(OH)_2$ as shown by the results of the FTIR test in Figure 2. However, on the XRD patterns, it only appears at a temperature of 1000°C.

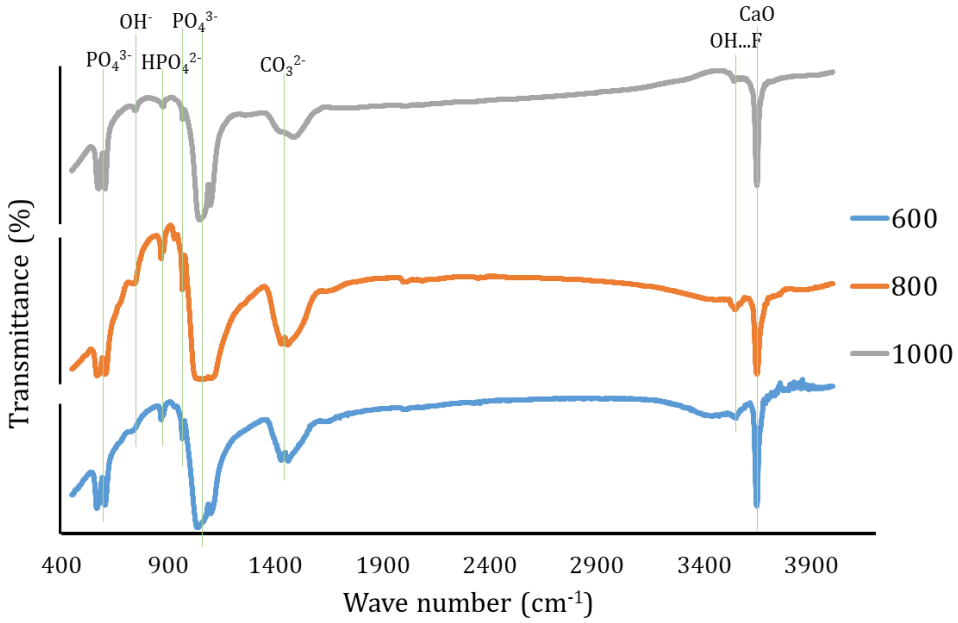

Figure 2. FTIR spectra for all samples with variations in sintering temperatures of 600°C, 800°C, and 1000°C.

3.2 FTIR Evaluation

The functional groups in the sample with three different sintering temperatures (600°C, 800°C, and 1000°C) are shown in Figure 2. All three samples show that they have the same functional groups. The infrared spectral assignments for fluorhydroxyapatite with various sintering temperatures are given in Table 1. Specific (OH...F) functional groups possessed by fluorhydroxyapatite from all samples can be observed around the wavenumber 3540 cm^{-1}. This shows that the hydroxyl group on hydroxyapatite was partially replaced with fluoride ion. OH-stretching mode shifts to the new band produced by a bond of OH...F. This proves that there is an interaction of OH...F in the compound [23]. Furthermore, the results of FTIR spectroscopy can be used to measure fluorine levels in the fluorhydroxyapatite sample [29]. The intensity of the stretch OH band in the region of 3480-3650 cm^{-1} can be used to measure fluorine levels in the fluorhydroxyapatite sample. The intensity of OH stretching band (s) in the 3480–3650 cm^{-1} region can be used to estimate the number of fluoride ions in fluorhydroxyapatite samples. At the concentrations of about 75% this band centers at 3547 cm^{-1}, while at the concentration of 50% and lower its center lies near 3541 cm^{-1}. The OH functional group ...F of the three samples appears at wavenumbers of 3548 cm^{-1}, 3546 cm^{-1}, and 3544 cm^{-1} which may indicate that at least 75% of the hydroxyl groups have been replaced by fluorine ions. This is in accordance with the ratio of concentrations of P and F used to obtain the chemical formula of fluorhydroxyapatite namely $Ca_{10}(PO_4)_6OH_{0.5}F_{1.5}$

There is a functional group of CaO at a wavenumber of approximately 3644-3646 cm^{-1} of all samples. The same was found in a similar study by Joughehdoust et al. [30]. His results also indicate the presence of CaO impurities in the synthesis of fluorhydroxyapatite. This data supports the x-ray data which shows the presence of CaO phase in all three samples.
In addition, the carbonate functional groups also appeared from the three samples around the wavenumber 1420 cm^{-1}. This is possible because of carbon dioxide contamination from the atmosphere towards the samples.

Table 1 Assignments and frequencies (in cm^{-1}) of bands in infrared spectra of Fluorhydroxyapatite with variations in sintering temperatures of 600°C, 800°C, and 1000°C.

Assignment	Infrared Frequency (cm^{-1}) of			
	Literature	600 °C	800 °C	1000 °C
OH^-	744 [31]	744	748	748
$v_3\ PO_4^{3-}$	1048 [31]	1039	1048	1048
$v_1\ PO_4^{3-}$	970 [31]	965	965	967
CO_3^{2-}	1473 [31]	1465	1476	1474
$v_4\ PO_4^{3-}$	568 [31]	566	566	576
$v_4\ PO_4^{3-}$	605 [31]	606	609	606
HPO_4^{2-}	870 [31]	868	867	878
CaO	3640 [32]	3644	3645	3646
OH...F	3546 [31]	3548	3544	3545

3.3 Conductivity Evaluation

Figure 3 shows the conductivity value of each sample. It can be seen that the higher the sintering temperature, the lower the conductivity of the sample. This shows that at higher purity of fluorhydroxyapatite, the conductivity value decreases, or it can be said that fluorhydroxyapatite material is a non-conductive material and therefore another treatment is needed to make fluorhydroxyapatite material become a conductive material. In addition, from all samples, it can also be seen that the conductivity increases with frequency. Theoretically, conductivity occurs because of ion jumps. In fluorapatite, the conduction mechanism is related to the release of fluoride ions along the c-axis in translation from the unit cell to the lattice in the interstitial state and back again. The fluoride ion must move to another position by forming a defect, where this defect can occur through thermal activity such as the Schottky defect which requires high activation energy due to the nature of the stoichiometric fluorapatite material [33].

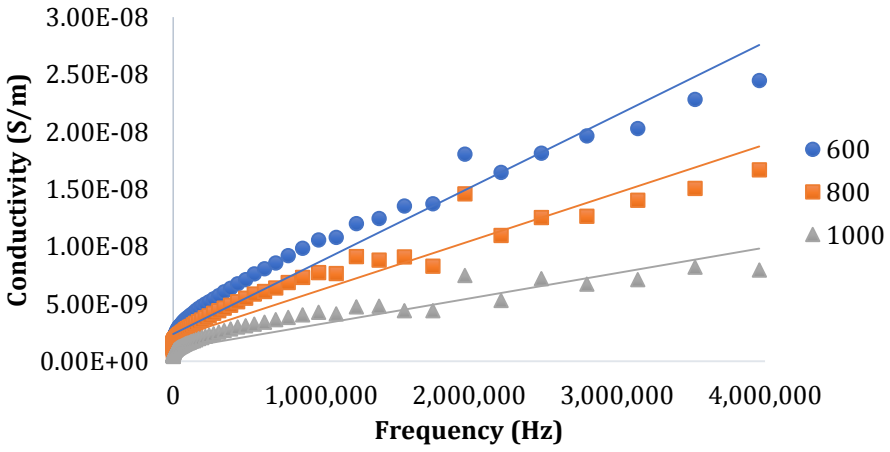

Figure 3. Conductivity as a function of frequency for three samples with variations in sintering temperature of 600 °C, 800 °C and 1000 °C.

At high frequency, conductivity and frequency have a linear relationship. This may be explained by the theory that the frequency response is in accordance with the resistor-capacitor (RC) model. The ion contained in the material is a complex network of the conductive and capacitive state. Conductivity analogous to a resistor that is independent of frequency, while the AC conductivity of the capacitive state is linearly related to the frequency (analogous to a capacitor, since $\sigma_{ac} = 2\pi f C$) [34].

3.4 SEM Analysis

The microstructure of the sample was observed through SEM testing results. Figure 4 shows the results of SEM micrographs. It can be seen that the morphology of the samples cannot be clearly seen due to agglomeration, but it can be observed that fluorhydroxyapatite is flat-shaped needle-like or rod-shaped. The same structure was found by Nathanael et al. [35] at the same temperature which is also rod-shaped. Sintering temperatures do not seem to affect the morphology. Research conducted by Khan et al. [36] at a temperature of 800°C and Eslami et al. [18] at a temperature of 1000°C, both produced rod-shaped fluorhydroxyapatite. Rod-like or needle-like shaped is needed because that shape that will fit in natural bone tissues [37].

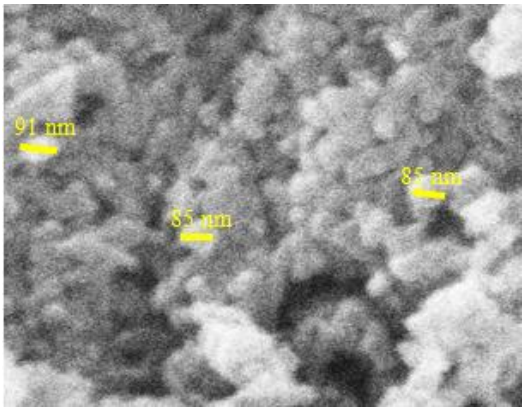

Figure 4. SEM micrograph for a sample with a sintering temperature of 600°C.

4. CONCLUSION

Fluorhydroxyapatite was synthesized through precipitation method and microwave assistant with varied sintering temperatures. The XRD results indicate that all samples show the presence of the fluorapatite phase but with different intensities. The samples sintered at higher sintering temperatures show that the fluorapatite phase dominates. The $Ca(OH)_2$ phase appears from the three samples. The $Ca(OH)_2$ phase in each sample decreases in intensity as the sintering temperature increases. The XRD results also show that at higher sintering temperatures, more fluoride ions replace the hydroxyl group. FTIR results show that the three samples have almost the same functional groups. Conductivity evaluation shows that the higher the sintering temperatures applied, the lower the conductivity value of the samples obtained. The morphology of the samples cannot be clearly seen due to the agglomeration. Despite that, it can be observed that fluorhydroxyapatite is flat-shaped needle-like or rod-shaped.

ACKNOWLEDGMENT

The authors show their appreciation and gratitude to Direktorat Riset dan Pengabdian Masyarakat, Direktorat Jenderal Penguatan Riset dan Pengembangan, Ministry of Research, Technology and Higher Education of the Republic of Indonesia for their funding to this research.

REFERENCE

[1] Fellah, B. H. & Layrolle, P. Sol-gel synthesis and characterization of macroporous calcium phosphate bioceramics containing microporosity. Acta Biomaterialia **5** (2009) 735-742.
[2] Aklil, A., Mouflih, M. & Sebti, S. Removal of heavy metal ions from water by using calcined phosphate as a new adsorbent. Journal of Hazardous Materials **112** (2004) 183-190.
[3] Bose, S. & Tarafder, S. Calcium phosphate ceramic systems in growth factor and drug delivery for bone tissue engineering: A review. Acta Biomaterialia **8**, **4** (2012) 1401-1421.
[4] Sharma, S. B., Sayyed, R. Z., Trivedi, M. H. & Gobi, T. A. Phosphate solubilizing microbes: sustainable approach for managing phosphorus deficiency in agricultural soils. Biomedical and Life Sciences **2** (2013) 1-14.
[5] Canal, C. & Ginebra, M. P. Fibre-reinforced calcium phosphate cements: A review. Journal of Mechanical Behaviour of Biomedical Materials **4** (2011) 1658-1671.
[6] Lin, K., Wu, C. & Chang, J. Advances in synthesis of calcium phosphate crystals with controlled size and shape. Acta Biomaterialia **10** (2014) 1-139.
[7] Ebrahimi-Kahrizsangi, R., Nasiri-Tabrizi, B. & Chami, A. Synthesis and characterization of fluorapatite–titania (FAp–TiO2) nanocomposite via mechanochemical process. Solid State Sciences **12** (2010) 1645-1651.
[8] Jarcho, M. Calcium Phosphate Ceramics as Hard Tissue Prosthetics. Clinical Orthopedics and Related Research **157** (1981) 259-279.
[9] Ramli, R. A., Adnan, R., Bakar, M. A. & Masudi, S. M.Synthesis and Characterisation of Pure Nanoporous Hydroxyapatite. Journal of Physical Science **22** (2011) 25-37.
[10] Dahlan, K. & Nuzulia, N. A. Synthesis of Chicken's Eggshell-Based B-Tricalcium Phosphate Bioceramics. Advanced Materials Research **1112** (2015) 458-461.
[11] Zou, C. *et al.* Preparation and characterization of porous b-tricalcium phosphate/collagen composites with an integrated structure. Biomaterials **26** (2005) 5276-5284.
[12] Yuan, H., Yang, Z., Li, Y. & ZHANG, X. Osteoinduction by calcium phosphate biomaterials. Journal Of Materials Science: Materials in Medicine **9** (1998) 723-726.
[13] Sasani, N., Ayask, H. K., Zebarjad, S. M. & Khaki, J. V. Characterization of Rod-like High-purity Fluorapatite Nanopowders Obtained by Sol-gel Method. Journal of Ultrafine Grained and Nanostructured Materials **46** (2013) 31-37.
[14] Fathi, M. H. & Zahrani, E. M. Fabrication and characterization of fluoridated hydroxyapatite nanopowders via mechanical alloying. Journal of Alloys and Compounds **475** (2009) 408–414.
[15] N, R. & Kumar, T. S. S. Synthesis of nanocrystalline fluorinated hydroxyapatite by microwave processing and its in vitro dissolution study. Bulletin of Material Science **29** (2006) 611-615.
[16] Fathi, M. H. & Mortazavi, V. S. Preparation and bioactivity evaluation of bone-like hydroxyapatite nanopowder. Journal of Materials Processing Technology **202** (2006) 536-542.
[17] Wei M., Evans, J.H. Bostrom, T. & Grondahl, L. Synthesis and Characterization of hydroxyapatite, fluoride-substituted hydroxyapatite and fluorapatite. Journal of Material Science: Material in Medicine **14** (2003) 311-320.
[18] Eslami, H., Hashjin, M. S. & Tahriri, M. Synthesis and characterization of nanocrystalline fluorinated hydroxyapatite powder by a modified wet-chemical process. Journal of Ceramic Processing Research **9** (2008) 224-229.
[19] Demnati, I. et al. Synthesis of fluor-hydroxyapatite powder for plasma sprayed biomedical coatings: Characterization and improvement of the powder properties. Powder Technology **255** (2014) 23-28.
[20] Kim, H. W., Kim, H. E. & Knowles, J. C. Fluor-hydroxyapatite sol–gel coating on titanium substrate for hard tissue implants. Biomaterials **25** (2004) 3351-3358.
[21] Legeros, R. Z., Silverstone, L. M., Daculsi, G. & Krebel, L. M. In vitro caries-like lesion formation in F-containing tooth enamel. Journal of Dental Research **62** (1985) 44-138.

[22] Lee, E.-J., Kim, H.-w. & Kim, H.-E. Biocompatibility of Fluor-Hydroxyapatite Bioceramics. Journal of the American Ceramic Society **88** (2005) 1309-1311.
[23] Shafiei, F. *et al.* Nanocrystalline fluorine-substituted hydroxyapatite [Ca5(PO4)3(OH)12xFx (0 ≤ x ≤ 1)] for biomedical applications: preparation and characterisation. Micro & Nano Letters **7** (2012) 109-114.
[24] Nikcevic, I. *et al.* Mechanochemical synthesis of nanostructured fluorapatite/fluorhydroxyapatite and carbonated fluorapatite/fluorhydroxyapatite. Journal of Solid State Chemistry **177** (2004) 2565-2574.
[25] Tredwin, C. J. *et al.* Hydroxyapatite, fluor-hydroxyapatite and fluorapatite produced via the sol-gel method: dissolution behaviour and biological properties after crystallisation. Journal of Material Science: Material in Medicine **25** (2014) 47-53.
[26] Hassan, M. N., Mahmoud, M. M., El-Fattah, A. A. & Kandil, S. Microwave-assisted preparation of Nano-hydroxyapatite for bone substitutes. Ceramic International **42** (2015) 1-10.
[27] Gross, K. A. & Rodriguez-Lorenzo, L. M. Sintered hydroxyfluorapatites. Part I: Sintering ability of precipitated solid solution powders. Biomaterials **25** (2004) 1375-1384.
[28] Tri Wahyudi S et al. Simple and Easy Method to Synthesize Chicken Eggshell Based Hydroxyapatite. Advanced Materials Research **896** (2014) 276-279.
[29] Baumer, A., Ganteaume, M. & Klee, W. E. Determination of OH ions in hydroxyfluorapatites by infrared spectroscopy. Bulletin de Minéralogie **108** (1985) 145-152.
[30] Joughehdoust, S., Behnamghader, A., Jahandideh, R. & Manafi, S. Effect ofaging temperature on formation of sol-gel derived Fluor-hydroxyapatite nanoparticles. Journal of nanosciences and nanotechnology **10** (2010) 2892-2896.
[31] Eslami, H., Solati-Hashjin & M. Tahriri, M., The comparison of powder characteristics and physicochemical, mechanical and The comparison of powder characteristics and physicochemical, mechanical and fluoridated hydroxyapatite. Materials Science and Engineering C **29** (2009) 1387–1398,
[32] Nasrazadani, S. & Eureste, E., Application of FTIR for Quantitative Lime Analysis. University of North Texas, Texas, (2008).
[33] Laghzizil, A. *et al.* Comparison of Electrical Properties between Fluoroapatite and hydroxyapatite materials. Journal of Solid State Chemistry **156** (2001) 57-60.
[34] Gittings, J. P. *et al.* Electrical characterization of hydroxyapatite-based bioceramics. Acta Biomaterialia **5** (2009) 743-754.
[35] Nathanael, A. J. *et al.* Influence of fluorine substitution on the morphology and structure of hydroxyapatite nanocrystals prepared by hydrothermal method. Materials Chemistry and Physics **137** (2013) 967-976.
[36] Khan, A. S. *et al.* Synthesis and characterizations of a fluoride-releasing dental restorative material. Materials Science and Engineering C **33** (2013) 3458-3464.
[37] Mollazade, S., Javadpour, J. & Khavandi, A. In situ synthesis and characterization of nano-size hydroxyapatite in poly(vinyl alcohol) matrix. Ceramics International **33** (2007) 1579-1583.